

***In situ* optical microscopy of the martensitic phase transformation of lithium**

M. Krystian and W. Pichl

Institut für Materialphysik der Universität Wien, Strudlhofgasse 4, A-1090 Wien, Austria

(Received 14 April 2000)

The phase transformation of lithium was investigated by *in situ* optical microscopy in a helium cryostat. The martensite microstructure is composed of irregular segments which grow in rapid bursts from many nuclei to a final size of 10 to 20 μm and then are immobilized. A major part of the segments is arranged in groups of parallel lamellas. A theoretical consideration of lattice compatibility predicts the existence of an almost perfectly coherent habit-plane interface between bcc and 9R in lithium. Therefore, the irregular microstructure is interpreted by the presence of the disordered polytype phase. Comparison with an earlier investigation in comparably impure lithium indicates a strong influence of impurities on the transformation mechanism. The connections between the low-temperature phase diagram, the geometrical compatibility condition, and the martensite microstructure are discussed.

I. INTRODUCTION

The low-temperature phase transitions of the alkali metals have been extensively studied by neutron-diffraction experiments during recent years.¹⁻⁹ They are characterized by complicated phase diagrams exhibiting the coexistence of different close-packed polytype structures. The low-temperature phase of Li is composed of a 9R (ABCBCACAB) together with a disordered polytype structure. Alloying pure Li with 10 at. % Mg suppresses the formation of the disordered polytype. In the solid solution only the 9R phase is observed.¹⁰ In contrast, severe plastic deformation of pure Li below the martensitic start temperature leads to a disintegration of the 9R phase into the disordered polytype.⁸ In Li as well as in Na the transformation is incomplete down to the lowest investigated temperatures. The low-temperature phase coexists with the parent bcc matrix. A recent Landau theory model¹¹ has explained the complex phase diagrams of the alkali metals by a coupling between the mechanisms corresponding to the *bcc*-9R, *bcc*-fcc and *bcc*-hcp transformations. In this picture fcc, hcp, and 9R play the roles of limit phases corresponding to critical values of the atomic shifts and associated with symmetry-breaking strains.

While neutron-scattering experiments and their subsequent theoretical interpretation have led to a thorough understanding of the phase diagrams of the alkali metals and of the transformation mechanisms on atomic scale, they did not yield information about the spatial distribution of the phases. The coexistence of several phases in martensitic transformations is usually associated with complex martensite-austenite microstructures. In particular, the occurrence of highly faulted or disordered polytype phases is frequently ascribed to geometrical incompatibility between the unfaulted martensite and the parent phase. Flat habit-plane interfaces between coexisting phases can only be formed for special critical ratios of the lattice constants which may be calculated from the so-called geometrically nonlinear theory of martensite microstructures.¹²⁻¹⁴ Deviations from the critical ratios result in a lattice mismatch which must be accommodated either by internal twinning or by internal faulting during the growth of

the martensite phase. This raises the question whether the tendency for formation of a disordered polytype phase in the alkali metals is an intrinsic property of the atomistic transformation mechanism, as suggested by the recent Landau theory model,¹¹ or a consequence of geometrical incompatibility between the lattices.

Experimental reports of the martensite microstructure and of the geometry and crystallography of the phase interface in the alkali metals have appeared very rarely in the literature. In contrast to the striking results obtained by neutron-scattering techniques, metallographic investigations have largely been inhibited by technical difficulties. Appropriate handling and preparation methods for the soft and highly reactive metals were not available until recently. Transmission electron microscopy and scanning electron microscopy investigations have not been performed at all. Only two early optical microscopy studies of the phase transformation of lithium have been reported in the 1950's. Hull and Rosenberg¹⁵ performed an *in situ* investigation in polycrystalline material without attempts for metallographic polishing of the surface. Bowles¹⁶ investigated the martensitic surface relief of single crystals at room temperature after the heating-cooling cycle. At this time it was not known that Li undergoes recrystallization subsequent to the reverse phase transformation¹⁷ and a major part of the surface relief is destroyed during heating to room temperature. Both investigations reported a microstructure of the low-temperature phase composed of planar lamellas. Bowles also determined the crystallographic orientation of the habit plane close to $\{441\}$.

We have recently developed improved metallographic preparation methods for alkali metals by chemical polishing under an inert atmosphere.¹⁸ In the present work we report on an optical microscopy investigation of the phase transformation of lithium single crystals which was performed *in situ* in a liquid-helium cryostat. It is shown that the low-temperature phase emerges from a large number of nuclei which grow to irregularly shaped segments of about 10 to 20 μm size and then become immobile. The segments are preferably arranged along flat lamellas, they are, however, also found dispersed in the bcc matrix. In the second part we study the lattice compatibility between the bcc and 9R

phases in Li on the grounds of the geometrically nonlinear theory of Hane and Shield.¹⁴ The theoretical calculation predicts an almost perfect compatibility between bcc and an *unfaulted* 9R phase which is in clear disagreement with the irregular microstructure observed in the experiment. It must be concluded that in contrast to the traditional view on martensitic transformations the severe faulting of the low-temperature phase of Li does not support the accommodation of lattice mismatch yet *inhibits* the formation of a flat habit-plane interface.

II. EXPERIMENT

High-purity Li single crystals of 10 mm diameter were grown by the method of combined vacuum distillation and Bridgman growth in one vessel.¹⁹ Handling and metallographic preparation were performed in a glove box under a protective atmosphere of highest-purity argon. For the investigation specimens were cut from the single-crystalline rods by spark erosion in an inert bath of mineral oil. The crystals were prepared for metallographic studies by a recently developed chemical polishing process in a sequence of high-purity organic solvents (butanol, acetone, benzene, diethylketone, and final cleaning in benzene in an ultrasonic cleaner which was operated inside the glove box). Details of the technique which yields an excellent mirrorlike surface are reported in Ref. 18. The polished crystals were mounted in a liquid-helium cryostat for optical microscopy which could be channeled into the glove box. Therefore, during their lifetime the samples never came into contact with the open atmosphere. Before the microscopy investigation the cryostat was mounted onto x-ray equipment for Laue transmission analysis. This determined the orientation of lattice directions with respect to the coordinate system of the microscope table.

III. EXPERIMENTAL RESULTS

A. First transformation and incubation times

In six virgin Li crystals cooled with average rates about 10 K/min the first traces of the martensite relief appeared in sudden bursts at 80 ± 2 K. In three other crystals the effect of isothermal holding above 80 K was studied in order to verify the recent observation of incubation times.⁷ At 85 K an incubated transformation occurred after 150 s. At 86 K the incubation time was 20 min. Isothermal holding at 90 K, however, induced a contrary effect. For over 3 h the crystal did not transform. During subsequent cooling, only at 50 K did traces of the martensite phase emerge. Down to 10 K the transformed fraction of the investigated surface was very small compared to all other crystals of the present investigation.

Figure 1 shows the surface of a Li crystal after the first transformation at 80 K. The plane of observation is close to $(013)_{\text{bcc}}$. Two straight lamellas of the martensite phase can be seen which are, however, composed of a substructure of irregular segments. During the transformation the lamellas did not form at once but the individual segments emerged in random order in a rapid sequence within a few seconds. In addition, Fig. 1 also shows isolated segments embedded in the bcc matrix. This characteristic microstructure was found in all investigated crystals. The structural units of the mar-

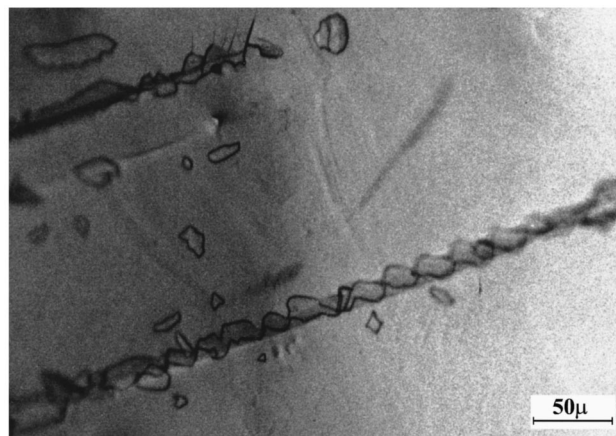


FIG. 1. Martensitic surface relief of a Li single crystal after the first transformation at 80 K. Plane of observation is close to (013) .

tensite phase are irregular segments of 10 to 20 μm size. The majority of them is arranged in planar lamellas, but they also appear dispersed in the matrix. It is obvious that the segments originate from numerous different nuclei.

At constant temperature the martensite microstructure formed in one sudden burst subsequently remains unchanged. Over several hours no indications of a further transformation could be detected. In contrast, even a minor temperature decrease of less than 1 K immediately induces new transformation bursts.

B. Cooling below the martensitic start temperature

During cooling the transformation permanently proceeds by burstlike nucleation of new martensite segments. In contrast, segments which are already present in the crystal do not further grow when the temperature is lowered. Examples of microstructures at different temperatures are shown in Figs. 2–4. The average shape and size of the segments was the same from 80 K to the lowest investigated temperatures (about 10 K). The majority of the segments was always concentrated in straight lamellas. Each of the investigated crystals exhibited three or four intersecting systems of parallel lamellas. One would suppose that they correspond to different symmetry-related variants of the 9R phase. The crystal-

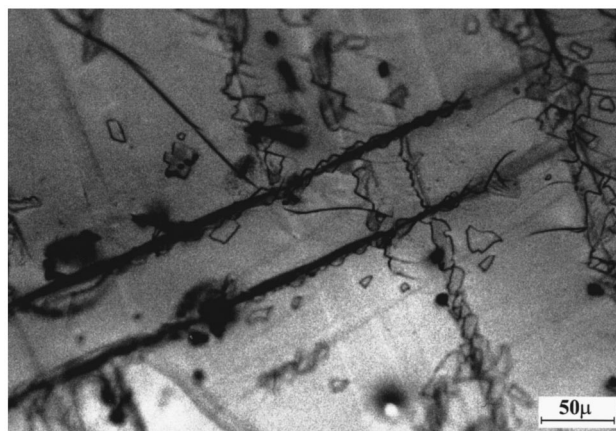


FIG. 2. Martensite microstructure at 70 K.

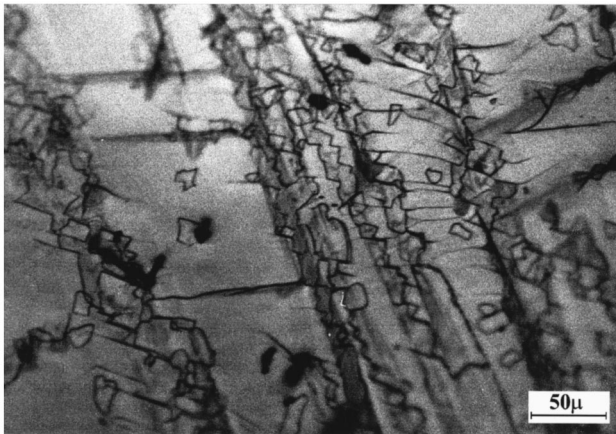


FIG. 3. Martensite microstructure at 60 K.

lographic trace analysis reported in Sec. IV, however, was in clear disagreement with this assumption.

Within the bcc matrix occasionally groups of parallel lines were observed, emanating from the martensite lamellas and either terminating in the matrix or interconnecting two neighboring lamellas. Examples can be seen in several parts of the Figs. 1–4. The lines must have their origin in an accommodation process of the matrix. Therefore, an interpretation as slip bands due to inhomogeneous plastic deformation seems to be obvious.

The lamellar microstructure of the martensite phase is essentially in agreement with the earlier investigations in Li.^{15,16} The pronounced substructure of irregular segments might have been overlooked in the earlier works due to a less perfect surface preparation. However, another striking discrepancy between the present and the earlier results, to be discussed in the following sections, indicates that there was in fact a fundamental difference in the transformation mechanism.

C. Reverse transformation and recrystallization

During heating from the low-temperature phase to room temperature the martensitic surface relief very gradually became diffuse and a major part finally disappeared. However, even at room temperature a few remainders of the relief could still be seen. The dissolution of the relief started about 120 K, i.e., in the range of the reverse transformation, and

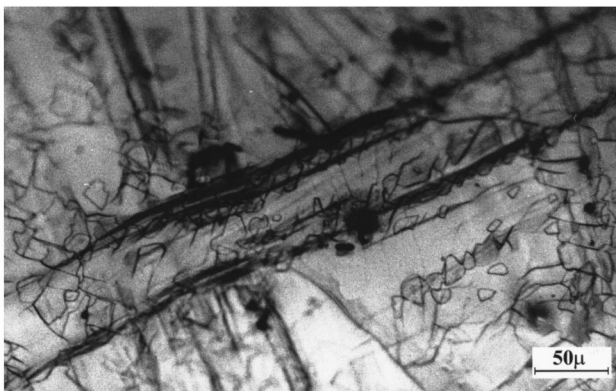


FIG. 4. Martensite microstructure at 50 K.

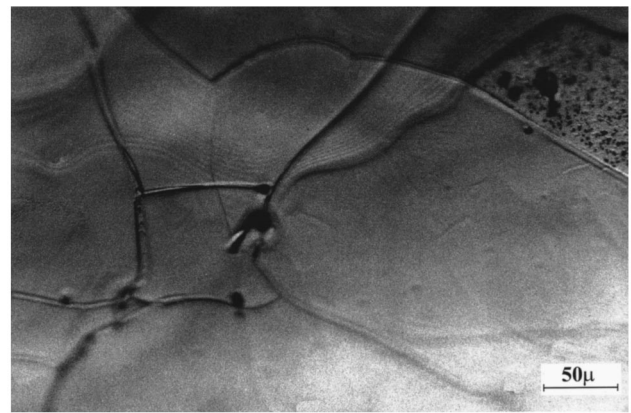


FIG. 5. Grain boundaries formed in the bcc single crystal by recrystallization subsequent to the reverse transformation.

was even more pronounced above 180 K where the reverse transformation is already complete. In particular, the reverse transformation did not give rise to a new type of relief. This shows that it is a very gradual process, in clear contrast to the burstlike transformation on cooling, and proceeds by shrinking of the low-temperature phase rather than by nucleation of the bcc structure inside the martensite. Such a thermoelastic behavior of the reverse transformation is in agreement with the fact that at 180 K a retransformed *single crystal* of the original orientation is again obtained.⁵

It is now well established from neutron scattering^{2,5} as well as from differential scanning calorimetry measurements¹⁷ that subsequent to the reverse transformation the retransformed Li single crystal disintegrates into a polycrystal by recrystallization. This process takes place in the temperature range between 200 and 230 K. Apart from the gradual dissolution of the martensitic relief, however, no indications of the nucleation and motion of grain boundaries could be observed *in situ* at the surface. This is not surprising. In contrast to martensitic phase transformations, recrystallization does not produce a surface relief. Grain boundaries usually can be observed only after etching. Indeed, a new chemical polishing of the retransformed crystals at room temperature clearly revealed the grain structure formed by recrystallization (Fig. 5). The x-ray Laue analysis also confirmed that the investigated samples had recrystallized.

It must be concluded that the gradual dissolution of the surface relief is not directly related to the reverse transformation or to the recrystallization mechanism. The occurrence of recrystallization, however, shows that in the designated temperature range various diffusion-controlled processes are strong, as also confirmed by recent measurements of the diffusion coefficient of Li below 200 K.²³ This strongly suggests that the release of the martensite relief is governed by a viscoplastic surface mechanism leading to a reduction of surface strains.

IV. CRYSTALLOGRAPHIC TRACE ANALYSIS

The irregular microstructure composed of many small segments shows that the usual concept of a habit-plane interface does not apply in Li. However, the average martensite lamellas seem to be extended on well-defined crystallographic planes, though these are not habit planes in the com-

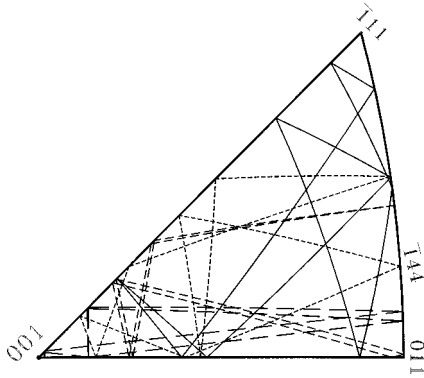


FIG. 6. One-surface trace analysis of martensite lamellas. 4 of 18 traces are shown. No common intersection point exists.

mon terminology. In order to determine the crystallographic orientation of these planes, attempts were made to evaluate the traces of the lamellas in a standard one-surface analysis. A two-surface analysis, which would allow an independent evaluation of individual lamellas, could not be performed since *in situ* rotation of the crystals in the helium cryostat was not possible. The one-surface analysis is based on the assumption that the planes of different systems of parallel lamellas are symmetry equivalent with respect to the parent-phase point group. This condition must necessarily be fulfilled if the traces correspond to different crystallographic variants of the low-temperature phase. The traces were plotted into a cubic standard projection and then reduced into one of the 48 unit triangles. A total of 18 traces from eight different crystals was evaluated (in Fig. 6, for clearness only four traces are shown). Surprisingly a common point of intersection did not exist, even if an error limit much larger than the resolution of the graphical evaluation method was admitted. This clearly shows that the basic assumption of the one-surface analysis is violated: the intersecting traces cannot be ascribed to different variants of the 9R phase.

The same method of trace analysis has been applied in the earlier investigation of Bowles.¹⁶ In his work all observed traces intersected close to the (441) pole which, therefore, was interpreted as the habit plane normal. In clear contrast, in the present investigation only 4 of 18 traces passed through (441). As we have shown above, there were some experimental imperfections in the work of Bowles since the traces were observed after warming to room temperature where a major part of the martensite relief had already disappeared. However, according to our own experience the remaining surface profile would be sufficient to perform a trace analysis. Therefore, the results of Bowles seem to be reliable. The discrepancy must be due to a major difference in the transformation mechanism which may also be reflected by the absence of the irregular substructure in the earlier work. In order to clarify this point, we studied the geometrical compatibility between the phases and calculated the theoretical habit plane for the bcc→9R transformation.

V. LATTICE COMPATIBILITY BETWEEN bcc AND 9R

In any martensitic transformation, a flat and coherent phase interface between the parent phase and a single variant of martensite must fulfill the habit plane equation¹⁴

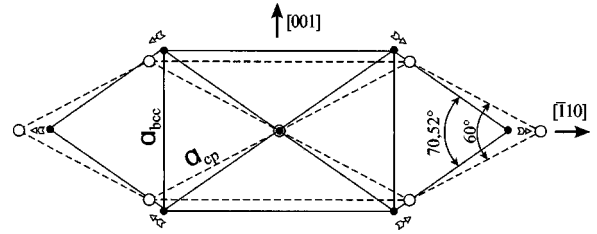


FIG. 7. Transformation of a (110)_{bcc} plane into a close-packed plane (first deformation of the Burgers mechanism).

$$RU - I = \mathbf{b} \otimes \mathbf{m}, \tag{1}$$

where U denotes the homogeneous deformation gradient tensor transforming one lattice into the other. I is the unity tensor. The unknowns are R , a rigid rotation determining the orientation relation between the phases, the habit plane normal \mathbf{m} , and the vector \mathbf{b} which is called the shape strain. By definition, U and R are the symmetric and the orthogonal part in the polar decomposition of the total deformation gradient

$$A = R \cdot U. \tag{2}$$

The necessary and sufficient conditions for the existence of solutions of Eq. (1) are

$$\lambda_1 \leq \lambda_2 = 1 \leq \lambda_3, \tag{3}$$

where λ_1 to λ_3 are the eigenvalues of U^2 , ordered with respect to their magnitude. Equation (3) represents the geometrical condition for the existence of a planar phase interface without accommodation by faulting or twinning. In general it is fulfilled only for special ratios of the lattice constants. If Eq. (3) holds, the solution for the habit plane normal, up to a normalization factor, is

$$\mathbf{m} = -\sqrt{1-\lambda_1} \mathbf{e}_1 \pm \sqrt{\lambda_3-1} \mathbf{e}_3, \tag{4}$$

where $\mathbf{e}_1, \mathbf{e}_3$ are the eigenvectors corresponding to the non-unity eigenvalues.

For the bcc→9R, bcc→hcp, and bcc→fcc transformations, the homogeneous lattice deformation U is obtained from the Burgers *two-deformation* mechanism²⁰ (we avoid the usual connotation *two-shear* mechanism since the first of the two deformations involves a small volume change). The first deformation changes the angle between two $\langle 111 \rangle_{\text{bcc}}$ directions within a common $\{110\}$ plane from 70.52° to 60° (Fig. 7) and adjusts the interplanar spacing of the close-packed planes to the experimentally observed value. In an orthonormal basis of axes parallel to $[110]_{\text{bcc}}, [\bar{1}10]_{\text{bcc}}, [001]_{\text{bcc}}$ it is given by the deformation gradient

$$U_1 = \begin{pmatrix} \frac{\sqrt{2}d_{cp}}{a_{bcc}} & 0 & 0 \\ 0 & \frac{\sqrt{3}a_{cp}}{\sqrt{2}a_{bcc}} & 0 \\ 0 & 0 & \frac{a_{cp}}{a_{bcc}} \end{pmatrix}, \tag{5}$$

where a_{bcc} is the bcc lattice constant, a_{cp} is the shortest lattice vector in the close-packed plane of the product lattice, and d_{cp} is the distance between neighboring close-packed

planes. The second deformation is a simple shear of the close-packed planes parallel to the direction corresponding to $[\bar{1}10]_{\text{bcc}}$, which generates the stacking sequence of the martensite phase. The additional atomic shuffle required to form a $9R$ or hcp structure from the bcc Bravais lattice does not contribute to the homogeneous lattice strain which occurs in the geometrical calculation. In the orthonormal basis defined above the gradient of the second deformation is

$$A_2 = \begin{pmatrix} 1 & 0 & 0 \\ \gamma & 1 & 0 \\ 0 & 0 & 1 \end{pmatrix}, \quad (6)$$

where $\gamma=1/9$ for the $\text{bcc} \rightarrow 9R$ transformation, $\gamma=1/3$ for $\text{bcc} \rightarrow \text{fcc}$ and $\gamma=0$ for $\text{bcc} \rightarrow \text{hcp}$. Other long-range ordered polytypes such as $18R$, $27R$, and $45R$ also correspond to specific values of γ . A_2 is not symmetric and therefore contains a rigid rotation. The pure lattice deformation U is obtained by splitting off the symmetric part from the product deformation gradient $A_2 \cdot U_1$ by the polar decomposition (2). (Note: the matrix product does not commute. The values of γ given above have been chosen for the designated order of the factors).

It should be noted that the calculation only relies on the total geometrical relation between the initial and the final lattice, as given by the Burgers mechanism. The splitting into two deformations is a convenient description, it does, however, not imply any assumption on the transformation path. If the first and the second deformation of the Burgers mechanism were in fact performed *one after the other*, an intermediate orthorhombic Bravais lattice (space group D_{2h}^{23}) would result, similar to the transformation model of Sankaran *et al.*²¹ In contrast, in the Landau theory model of Ref. 11 the atomic shuffle was identified as the primary order parameter for the $\text{bcc} \rightarrow \text{hcp}$ and $\text{bcc} \rightarrow 9R$ transformations, which leads to intermediate phases D_{2h}^{17} and C_{2h}^3 , respectively. For the $\text{bcc} \rightarrow \text{fcc}$ transformation the total lattice deformation U from the Burgers mechanism is equivalent to the well-known Bain deformation.²²

For the calculation of the $\text{bcc} \rightarrow 9R$ transformation in Li we used the lattice constants reported from neutron measurements:² $a_{\text{bcc}}=3.483 \text{ \AA}$, $a_{9R}=3.103 \text{ \AA}$, and $d_{9R}=2.533 \text{ \AA}$. The resulting eigenvalues of U^2 are $\lambda_1=0.794$, $\lambda_2=0.993$, $\lambda_3=1.269$. This shows that the compatibility condition (3) is fulfilled within very good accuracy and hence the lattice mismatch is extremely small. Therefore, in Li an almost perfectly coherent phase interface between bcc and an unfaulted and untwinned $9R$ structure should exist. From Eq. (4) the indices of the habit plane normal, transformed to the cubic standard basis, are (3.94, 4.38, 1), close to the value (441) observed by Bowles. Such a coherent interface would be highly mobile since almost no accommodation strains are required. Therefore, long, straight martensite lamellas should easily grow from one nucleus. This is in clear disagreement with the irregular microstructure observed in the present investigation which evolves from a large number of nuclei.

The evaluation of Eq. (1) also yields the rigid rotation R and therefore makes a theoretical prediction of the orientation relation. Following the calculation procedure of Ref. 14,

we obtain the relation $(009)_{9R} \parallel (0.914, 1.021, 0.070)_{\text{bcc}}$. Excellent agreement with the experimental observations of Berliner *et al.*,⁴ who have reported the position of the $(009)_{9R}$ reflection at $(0.92, 1.018, 0.06)_{\text{bcc}}$, confirms that the Burgers mechanism provides an adequate geometrical description of the $\text{bcc} \rightarrow 9R$ transformation in Li.

Similar calculations were performed for hypothetical transformations to other polytypes, using the experimental lattice constant values of Li. While for the $\text{bcc} \rightarrow 9R$ transformation the deviation of the eigenvalue λ_2 from unity is only 0.7%, for hcp, $18R$, and $27R$ polytypes it ranges from 2 to 3%. The strongest lattice mismatch is found for the fcc structure where the deviation is more than 5% (in this latter calculation only a_{cp} can be adjusted to the experimental value while d_{cp} is fixed by the cubic symmetry of the product phase). This shows that the $9R$ phase is the *geometrically* most favorable low-temperature structure. The heavy faulting observed in neutron investigations, however, indicates that it is not the *thermodynamic* equilibrium phase.

VI. DISCUSSION

The preceding geometrical analysis shows that the earlier microstructure observations of Bowles are in close agreement with a transformation mechanism from bcc to a *perfect* $9R$ phase. Therefore, it must be concluded that our contrary results are due to the presence of the disordered polytype phase which inhibits the evolution of the coherent {441} habit-plane interface predicted by the geometrical theory for pure $9R$. The failure of the trace analysis clearly demonstrates that the different systems of parallel martensite lamellas are not related by cubic symmetry and hence cannot be attributed to crystallographic variants of the $9R$ phase. This suggests that they correspond to stacking variants within the disordered polytype phase, distinguished by different mesoscopic average stacking sequences and thus by different average values of the shear parameter γ in Eq. (6). The four traces which intersected in the (441) pole might represent variants of a perfect $9R$ phase, though this cannot be directly proved at present. A martensite segment growing from one nucleus with a certain average stacking sequence seems to trigger the formation of other segments of similar stacking (similar average values of γ) in the vicinity by its anisotropic strain field. This leads to the autocatalytic chain reaction observed during the transformation bursts which is responsible for the preferred concentration of the segments along straight lamellas.

The question arises why the disordered polytype phase was absent in the earlier work of Bowles. A major difference between our present Li crystals and those investigated by Bowles concerns the purity. The vacuum distillation technique used in the present investigation reduces the impurity content of the Li material to a few ppm (with the only exception of being the element Na which may be one order of magnitude higher, see Ref. 19 for details). On the other hand, Bowles reported a purity of his crystals of 99.86%, which is even worse than our starting material for the distillation. Therefore, the diverging results strongly indicate that an increased concentration of foreign atoms suppresses the formation of the disordered polytype and favors the perfect $9R$ phase. This is corroborated by neutron investigations in

Li-Mg alloys¹⁰ where also the disordered polytype phase does not exist and the low-temperature structure is pure $9R$.

Impurities seem to have a major influence also on other features of the phase transition of Li. Strong controversies have appeared in the literature concerning a softening of the Σ_4 phonon branch as a precursor of the transformation. In inelastic neutron-scattering measurements by Blaschko and co-workers^{1,5} between 200 and 100 K a partial softening of the branch extending from $\mathbf{k}=0.1[110]$ to the zone boundary was observed. Between 100 and 80 K a small dip near $1/3[110]$ formed. In the investigations of Smith and co-workers^{2,6} this dip was absent. The Landau theory model of Ref. 11 could partially reconcile the controversial results. It was shown that the presence or absence of the dip can be explained by a different transformation path which was close to the stability regime of the intermediate Landau phase in the crystals of Blaschko *et al.*, while it was far from this regime in the investigations of Smith *et al.* In our opinion, these different transformation paths might have their origin also in a small difference of the impurity content. Both research groups used a pure ^7Li isotope as starting material for crystal growth. As a consequence of the isotope separation process, the concentration of foreign chemical elements in this material is naturally very small. However, the single crystals investigated by Blaschko and co-workers were additionally purified by the same vacuum distillation technique used in the present work. Presumably, therefore, there was a minor difference in the chemical composition which might be responsible for the controversial transformation behavior.

VII. SUMMARY AND CONCLUSIONS

The essential results of the present investigation are summarized as follows:

(1) The martensite phase of high-purity lithium is composed of irregular segments of 10 to 20 μm size which grow from a large number of nuclei. A major part of the segments assembles along planar lamellas, though they also occur dispersed in the bcc matrix.

(2) The segments grow to their final size in a rapid burst and then are immobilized. On cooling the transformation proceeds by nucleation of new segments, not by growth of already existing ones.

(3) Different groups of parallel martensite lamellae cannot be attributed to crystallographic variants of the $9R$ phase. It is suggested that they correspond to variants of the disordered polytype phase distinguished by different mesoscopic average stacking sequences.

(4) A calculation from geometrical martensite theory shows that the bcc and the unfaulted and untwinned $9R$ phase in Li are almost perfectly compatible without lattice mismatch. A coherent habit-plane interface close to $\{441\}$ is predicted. This has in fact been observed in an earlier investigation in rather impure lithium. In contrast, in high-purity Li the presence of the disordered polytype phase seems to inhibit the formation of this coherent interface and leads to the irregular microstructure found in the present investigation. It is concluded that impurity atoms suppress the disordered polytype and enhance the transformation to a perfect $9R$ structure.

(5) The geometrical calculation also determines the crys-

tallographic orientation relation between bcc and $9R$. The irrational relation observed in neutron diffraction is derived within excellent accuracy.

(6) Between 80 and 86 K an incubation of the transformation up to 20 min was observed. In contrast, isothermal holding at 90 K leads to a partial suppression of the phase transition. The origin of this change of the behavior between 86 and 90 K is rather unclear at present and should be separately investigated.

(7) The reverse transformation is a smooth thermoelastic process which does not produce any marks at the surface. The occurrence of recrystallization subsequent to the reverse transformation was confirmed.

The present results have demonstrated the close connections between the complex phase diagram, the geometrical lattice compatibility condition and the martensite microstructure of Li. In summary, the following interpretation is suggested which is essentially in agreement with the model of Ref. 11. Below 180 K, the thermodynamic equilibrium phase is fcc which in reality only occurs on heating.³ The fcc phase cannot nucleate from the parent bcc phase due to severe lattice mismatch. However, nucleation fluctuations may be present in the undercooled bcc structure. This would be in agreement with the softening of almost the entire Σ_4 phonon branch between 200 and 100 K. Recently it has also been shown that a pronounced anomaly of the diffusion coefficient in the same temperature range can be attributed to such fluctuations.²³ Between 100 and 80 K the enthalpy difference between fcc and $9R$ decreases, i.e., the fluctuations become more $9R$ -like on the average. This may be the origin of the controversial dip in the Σ_4 branch. Finally, at 80 K the highly faulted $9R$ phase nucleates in a sudden burst from many fluctuations. This fluctuation-driven nucleation mechanism is in agreement with the observation of incubation times. The average stacking sequence as well as the final size of the martensite segments are determined by a balance between the thermodynamic driving force favoring an fcc stacking and the necessity to form a mobile phase interface which favors the geometrically most suitable $9R$ structure. The above-mentioned autocatalytic triggering leads to a microstructure of parallel lamellas which correspond to disordered polytype variants of specific mesoscopic average values of the shear parameter γ . The $9R$ phase may be localized in lamellas which are extended on $\{441\}$ planes, corresponding to a value $\gamma=1/9$. On heating the thermodynamically stable fcc phase, which cannot nucleate from the parent bcc lattice, is formed from the disordered polytype by an ordering-type phase transition.¹¹ The final thermoelastic reverse transformation fcc \rightarrow bcc occurs by shrinking of the fcc phase, not by nucleation of bcc. Such a mechanism *on heating* requires a high interface mobility and at first sight, therefore, seems to be in contradiction to the strong lattice misfit between bcc and fcc which inhibits the nucleation of fcc *on cooling*. There are, however, indications that the motion of the extended interface in this temperature range may be supported by diffusion. Heat flux curves from differential scanning calorimetry¹⁷ have revealed a significant overlap between the final reverse transformation and the onset of the subsequent recrystallization process. This suggests that the fcc \rightarrow bcc reverse transformation is not a true martensitic transformation but at least partially diffusion driven.

ACKNOWLEDGMENTS

We are indebted to Dr. A. Fuith and Dr. H. Kabelka who made us available their helium cryostat for optical micros-

copy. Many thanks to Dr. G. Krexner and Professor P. Tolédano for helpful discussions. The work was supported by the Austrian Fonds zur Förderung der wissenschaftlichen Forschung (Project No. P12990-PHY).

-
- ¹G. Ernst, C. Artner, O. Blaschko, and G. Krexner, *Phys. Rev. B* **33**, 6465 (1986).
- ²H. G. Smith, *Phys. Rev. Lett.* **58**, 1228 (1987).
- ³W. Schwarz and O. Blaschko, *Phys. Rev. Lett.* **65**, 3144 (1990).
- ⁴R. Berliner, H. G. Smith, J. R. D. Copley, and J. Trivisonno, *Phys. Rev. B* **46**, 14 436 (1992).
- ⁵W. Schwarz, O. Blaschko, and I. Gorgas, *Phys. Rev. B* **44**, 6785 (1992).
- ⁶H. G. Smith, R. Berliner, and J. Trivisonno, *Phys. Rev. B* **49**, 8547 (1994).
- ⁷Ch. Maier, O. Blaschko, and W. Pichl, *Phys. Rev. B* **52**, 9283 (1995).
- ⁸Ch. Maier, O. Blaschko, and W. Pichl, *Phys. Rev. B* **55**, 113 (1997).
- ⁹Ch. Maier, O. Blaschko, and W. Pichl, *Phys. Rev. B* **55**, 12 062 (1997).
- ¹⁰Ch. Maier, R. Glas, O. Blaschko, and W. Pichl, *Phys. Rev. B* **51**, 779 (1995).
- ¹¹O. Blaschko, V. Dmitriev, G. Krexner, and P. Tolédano, *Phys. Rev. B* **59**, 9095 (1999).
- ¹²J. M. Ball and R. D. James, *Arch. Ration. Mech. Anal.* **100**, 13 (1987).
- ¹³J. M. Ball and R. D. James, *Philos. Trans. R. Soc. London, Ser. A* **338**, 389 (1992).
- ¹⁴K. F. Hane and T. W. Shield, *Philos. Mag. A* **78**, 1215 (1998).
- ¹⁵D. Hull and H. M. Rosenberg, *Cryogenics* **1**, 27 (1960).
- ¹⁶J. S. Bowles, *Trans. AIME* **191**, 44 (1951).
- ¹⁷W. Pichl, *Phys. Status Solidi A* **158**, 101 (1996).
- ¹⁸M. Krystian and W. Pichl, *Mater. Char.* (to be published).
- ¹⁹W. Pichl and M. Krystian, *Phys. Status Solidi A* **160**, 373 (1997).
- ²⁰W. G. Burgers, *Physica (Amsterdam)* **1**, 56 (1934).
- ²¹H. Sankaran, S. M. Sharma, and S. K. Sikka, *J. Phys.: Condens. Matter* **4**, L61 (1991).
- ²²E. G. Bain, *Trans. AIME* **70**, 25 (1924).
- ²³A. Seeger, O. Wieland, H. D. Carstanjen, W. Frank, and M. Neumann, in *Proceedings of the International Conference on Solid-Solid Phase Transformations*, Kyoto, 1999, edited by M. Koiwa, K. Otsuka, and T. Miyakazi (Japan Institute of Metals, Kyoto, 1999), p. 449.